Proceedings of the ASME 2017 Fluids Engineering Division Summer Meeting
SAND2017-4297C
FEDSM2017
July 30-August 3, 2017, Waikoloa, HI, USA

FEDSM2017-69023

GAS-INDUCED MOTION OF AN OBJECT IN A LIQUID-FILLED HOUSING DURING VIBRATION: II. EXPERIMENTS

Timothy J. O'Hern, John R. Torczynski, Jonathan R. Clausen, Timothy P. Koehler
Sandia National Laboratories
Albuquerque, NM 87185 USA

ABSTRACT

We develop an idealized experimental system for studying how a small amount of gas can cause large net (rectified) motion of an object in a vibrated liquid-filled housing when the drag on the object depends strongly on its position. Its components include a cylindrical housing, a cylindrical piston fitting closely within this housing, a spring suspension that supports the piston, a post penetrating partway through a hole through the piston (which produces the position-dependent drag), and compressible bellows at both ends of the housing (which are well characterized surrogates for gas regions). In this system, liquid can flow from the bottom to the top of the piston and vice versa through the thin annular gaps between the hole and the post (the inner gap) and between the housing and the piston (the outer gap). When the bellows are absent, the piston motion is highly damped because small piston velocities produce large liquid velocities and large pressure drops in the Poiseuille flows within these narrow gaps. However, when the bellows are present, the piston, the liquid, and the bellows execute a collective motion called the Couette mode in which almost no liquid is forced through the gaps. Since its damping is low, the Couette mode has a strong resonance. Near this frequency, the piston motion becomes large, and the nonlinearity associated with the position-dependent drag of the inner gap produces a net (rectified) force on the piston that can cause it to move downward against its spring suspension. Experiments are performed using two variants of this system. In the single-spring setup, the piston is pushed up against a stop by its lower supporting spring. In the two-spring setup, the piston is suspended between upper and lower springs. The equilibrium piston position is measured as a function of the vibration frequency and acceleration, and these results are compared to corresponding analytical results (Torczynski et al., 2017). A quantitative understanding of the nonlinear behavior of this system may enable the development of novel tunable dampers for sensing vibrations of specified amplitudes and frequencies.

INTRODUCTION

The motion of a piston in a vibrated liquid-filled cylindrical housing can be dramatically changed by introducing a small amount of gas (Torczynski et al., 2014, 2015, 2016, 2017; O'Hern et al., 2016a,b,c; Romero et al., 2016). Photographs of such a system with vibration off and on are shown in Fig. 1, and its cross section is shown schematically in Fig. 2a. The piston is supported against gravity by a helical wire spring, and the piston has a circular hole along its axis, into which a post fixed to the housing protrudes partway. Thus, the flow resistance of the gap between the adjacent surfaces of the piston and the post varies with the piston's vertical position. This inner gap and the outer gap between the piston and the housing are both narrow, so any piston motion that forces liquid through these gaps is highly damped (Asami et al., 2014). Under certain vibration conditions, some gas from above the piston migrates downward and becomes trapped below the piston by Bjerknes forces (Bjerknes, 1906; Romero et al., 2014). When gas regions exist both above and below the piston, the piston can move downward against its supporting spring during vertical vibration.

In this paper, we experimentally investigate how the presence of gas regions above and below the piston can change the dynamics so as to cause the piston to move downward during vertical vibration and how the piston and post geometry affect this rectified motion. Herein, we do not investigate in detail how the lower gas region is formed but instead focus on the effect of the two gas regions once they exist. Following the pioneering work of Bjerknes (1906), many investigators have studied the downward rectified motion of a gas bubble in a vibrated liquid. Most researchers have focused on a small isolated spherical bubble in a large open geometry, but relatively few researchers have investigated the formation and stability of a lower gas region in a highly confined geometry like the ones in Figs. 1-2. An extensive bibliography for downward rectified bubble motion is given elsewhere (Romero et al., 2014).

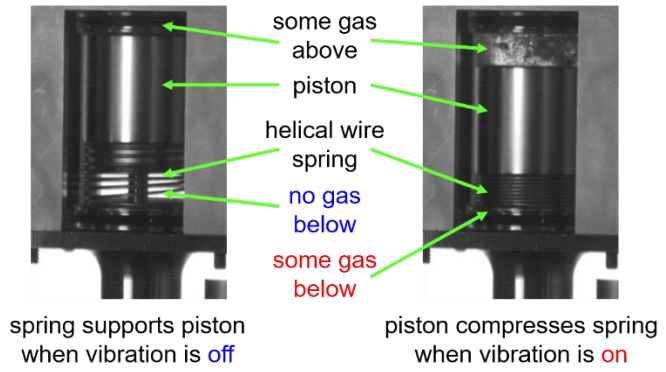

Figure 1. Multiphase dynamical system under investigation. Photographs of an experiment showing that vertical vibration can cause a piston in a liquid-filled housing with some gas present to move downward and compress its supporting helical wire spring (Romero et al., 2016).

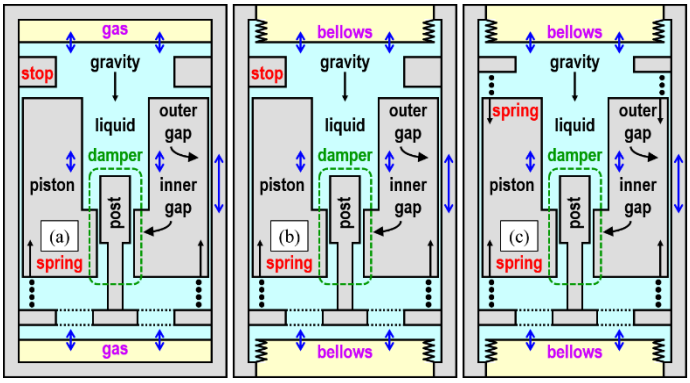

Figure 2. Schematic cross sections of the systems studied herein (Torczynski et al., 2015, 2016; O'Hern et al., 2016a,b,c). Left (a): Single-spring setup with piston pushed up by lower spring against stop like Fig. 1; compressible regions are gas. Middle (b): Single-spring setup with piston pushed up by lower spring against stop; compressible regions are bellows. Right (c): Two-spring setup with piston suspended between lower and upper springs; compressible regions are bellows. Actual gaps are much narrower than those depicted above. Piston is shown at zero-force position, which is half-aligned. Length of inner gap depends linearly on the piston position.

Here, we analyze the effect of these gas regions by studying systems like the two shown schematically in Fig. 2b and Fig. 2c. In these surrogate systems, the upper and lower gas regions are replaced by bellows with similar pressure-volume relationships. Thus, the effect of the gas (pneumatic) spring formed by these compressible regions can be analyzed in isolation without the additional complexity of downward gas migration. It is essential to have two compressible regions (gas or bellows), one above and the other below the piston because a single compressible region in an incompressible fluid cannot undergo a volume change and thus cannot produce a pneumatic spring. In our analysis (Torczynski et al., 2017), the geometry is taken to be axisymmetric, and the piston is allowed to move only in the vertical direction. The latter assumption is justified because the outer gap is narrow relative to the piston diameter for realistic situations (Asami et al., 2014; Torczynski et al., 2014, 2015).

Many researchers have studied the motion of a rigid body in a viscous liquid during vibration. An extensive bibliography for this topic is given elsewhere (Romero et al., 2016). Generally, the rigid body is a small particle in a large housing, which is the opposite of the present situation. An exception is the numerical study of oil dampers by Asami et al. (2014). Along with the gas (pneumatic) spring produced by the two gas regions, the position-dependent drag on the piston is the other factor essential for explaining the phenomena investigated herein.

The companion paper (Torczynski et al., 2017) presents additional background and theoretical and computational work for this system. They show how the addition of compressible regions can change the system dynamics from the highly damped Poiseuille mode, with high drag in the flow through narrow gaps, to a low-damping collective motion termed the Couette mode.

EXPERIMENTS

Two test cells are used here. The first is the single-spring setup of Fig. 2b, which has an internal geometry like Figs. 1-2a but which has bellows instead of gas regions above and below the piston. The second is the two-spring setup of Fig. 2c, which is identical to the single-spring setup except that the upper stop is replaced by an upper spring. In both setups, the open internal volume is completely filled with 20-cSt polydimethylsiloxane (PDMS) silicone oil (Clearco, 2017), with density 950 kg/m^3 and viscosity 0.019 kg/(m s). No air is present in the open volume.

The single-spring test cell has the following components. A 22.86-mm-diameter cylinder is bored into a clear acrylic block. The cylinder contains a stainless steel piston, a post, and a spring, with a 0.0508-mm radial gap between the piston and the cylinder. The spring has a spring constant of 38 N/m. Two bellows of average diameter 2.184 cm, total effective mass 0.0086 kg, and total spring constant 18,534 N/m are mounted at the top and bottom of the cylinder. The spring pushes the piston up against a stop. A hole of inner diameter 9.525 mm passes through the piston, and a post of diameter 3.988 mm fixed to the housing penetrates partway into this hole. Matching protrusions of length 5.080 mm from the post and the hole form an inner gap of mean diameter 5.004 mm and radial height 0.127 mm. The length of this gap decreases linearly as the piston moves downward from the fully-aligned position (where the piston and post protrusions align) to the anti-aligned position (where the top of the piston protrusion is aligned with the bottom of the post protrusion).

The two-spring test cell, shown in Fig. 3, is like the single-spring test cell except that it uses two springs to suspend the piston away from the stop. The piston is stainless steel and has a mass 0.0728 kg. The two springs have a total spring constant of 70 N/m. The zero-force position, at which gravity, buoyancy, and spring forces sum to zero, is close to the half-aligned position.

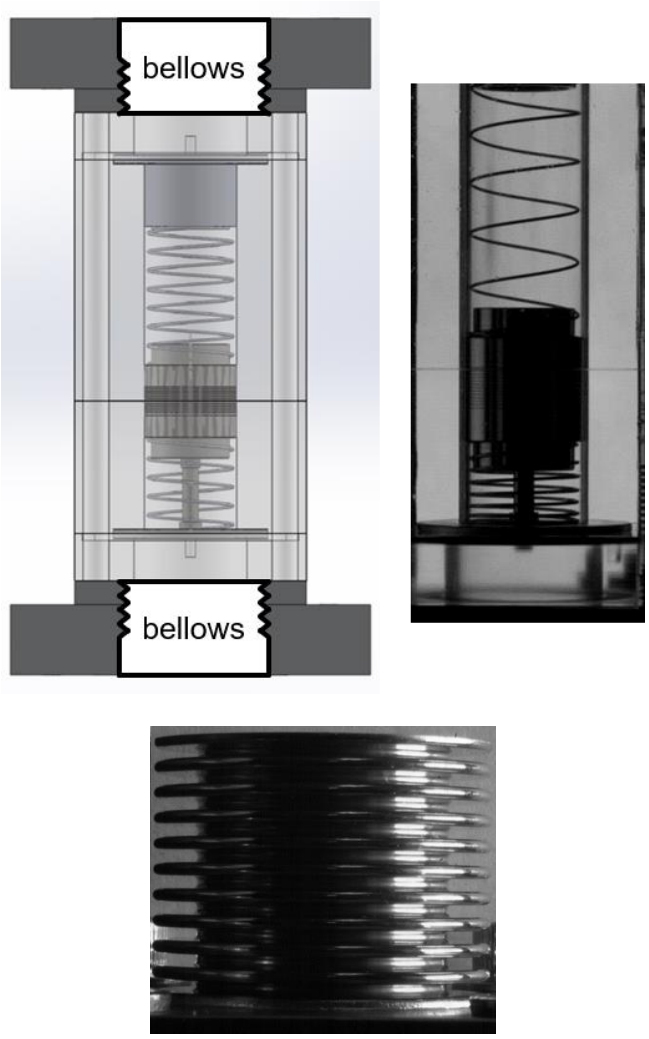

Figure 3. Two-spring test cell (see Fig. 2c). Top left: schematic diagram. Top right: photo. Springs above and below piston suspend it in the liquid and prevent it from contacting stop. Bottom: close-up photo of bellows used in both test cells.

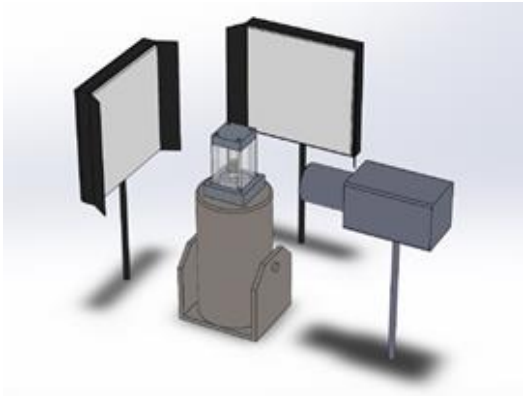

Figure 4. Experimental setup. Test cell is subjected to vertical vibration by shaker. Camera tracks piston motion. Test cell is backlit with a diffuse LED array light source.

The bellows used in both test cells are shown in Fig. 3. Servometer Model FC-16 electroformed bellows, with nominal outer diameter 25.4 mm (Servometer, 2015), are used because their pressure-volume relationship is similar to 1.5 mL bubbles. These bellows are welded to base plates, which are attached to the top and bottom of the test cell. The spring constant, resonance, and damping of each bellows was measured both with a commercial texture tester and by finding its resonant frequency with different attached masses.

Experiments are performed by mounting a test cell on an electrodynamic shaker and subjecting it to a controlled vibration. Piston motion is monitored by several cameras. Figure 4 is a simplified schematic diagram of the setup. The piston is initially near the half-aligned position, the vibration acceleration and frequency are selected, and the piston position is recorded. This procedure allows the equilibrium piston position to be determined for a wide range of vibration conditions.

A Labworks Model ET-140 electrodynamic shaker is used, and a LabVIEW program is used to control the shaker and to record the vibration acceleration and frequency, as well as the time-resolved piston position. The housing motion is measured using a PCB Piezoelectronics uniaxial accelerometer. This accelerometer signal is used in a PI feedback loop to maintain the prescribed sinusoidal vibration conditions. The vibration control parameters are the acceleration and the frequency, from which the displacement is found.

Piston position is found using an Allied Vision Technologies Manta GigE camera with a LabVIEW edge tracking routine. Images are recorded using a Phantom v9.1 high-speed camera, typically run at 1000 frames/second. The test cell is backlit with a diffuse LED array light source (Fig. 4).

Error sources in this experiment include the accelerometer that measures the vibration conditions and the edge finding algorithm used to track the piston motion. The accelerometer is a PCB miniature ceramic shear accelerometer 352A24 with accuracy specifications of ±5% on frequency and ±10% on acceleration. The edge tracker is accurate to ±1 pixel, which is ±0.045 mm for the magnification used in these experiments.

Experiments are performed at frequencies of 20-200 Hz and accelerations of 0.1-20g (0.98-196 m/s^2), with displacements of 0.004-1.5 mm. Experimental variables include the vibration conditions and the inner-gap geometry. Of special interest is the effect of the stop, which is present in the single-spring test cell (Fig. 2b) but is absent in the two-spring test cell (Fig. 2c). All experiments are performed at room temperature and pressure.

Figure 5 shows the piston position determined from image analysis for the single-spring test cell (Fig. 2b) at 13g and 60 Hz. The piston oscillates rapidly while drifting downward gradually from its initial position (near the half-aligned position) to its final equilibrium position (near the anti-aligned position). This final state is denoted as either “up” or “down” depending on whether the final equilibrium position is near the half-aligned position or the anti-aligned position, respectively. Thus, as in Fig. 5, the final state of the piston at 13g and 60 Hz is down.

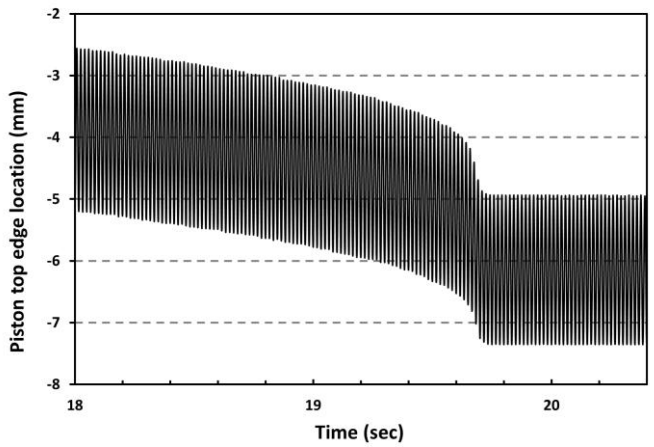

Figure 5. Portion of time trace of piston motion at 13g and 60 Hz in single-spring test cell. Piston oscillates rapidly and drifts down gradually from its initial positon (near half-aligned) to its final "down" equilibrium position (near anti-aligned).

Figure 6 is a regime map for the single-spring test cell that is built up from many cases like the one shown in Fig. 5 for accelerations of 0.5-10g and frequencies of 40-200 Hz. Experimental results acquired as above are compared to results from a previously developed theory (O'Hern et al., 2016a). In the theory, the piston is up or down depending on whether the rectified force pushing the piston down is less than or greater than the spring force pushing the piston up. Near the resonant frequency of 107 Hz, the piston oscillation becomes large, and the rectified force becomes correspondingly large, so the piston moves to the down state even for low values of the acceleration.

In the experiments, however, the piston stays in the up state over the entire frequency range for all accelerations below some critical value in the 7-10g range. For an acceleration above this critical value, as the frequency is increased, a critical frequency is reached above which the piston moves to the down state. The piston then stays in the down state as frequency continues to increase. When some yet higher critical frequency is reached, the piston returns to the up state. Thus, for the given acceleration, the "piston-down" regime is bounded by these lower and higher critical frequencies and the critical acceleration. The frequency range decreases as the acceleration is decreased and vanishes when the acceleration falls below the critical acceleration value (in the 7-10g range for the conditions in Fig. 6).

Unfortunately, two identical experiments yield different piston-down regimes. Although their left and right frequency boundaries are similar, their critical accelerations below which the piston always stays up differ significantly. Unlike the experimental regime boundary, the theoretical regime boundary has no critical acceleration: the acceleration needed for the piston to move to the down state becomes quite small near the resonant frequency of 107 Hz, as mentioned above. The interaction of the piston with the stop, inherently present in the experiment but not treated in the theory, is presumed to cause this difference.

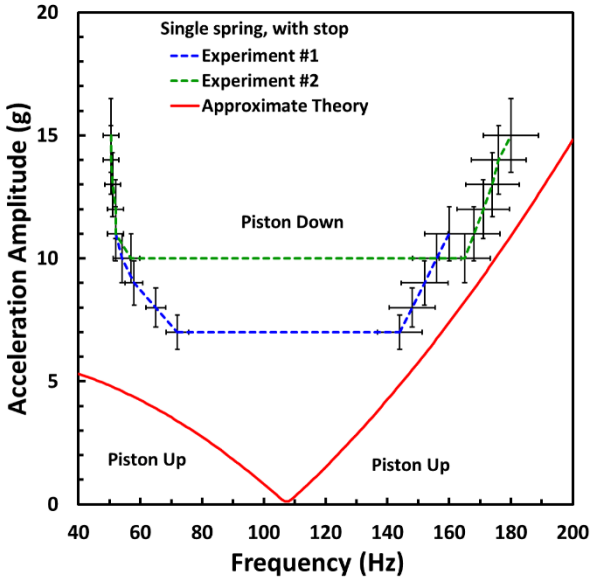

Figure 6. Regime map of piston equilibrium state (down or up) versus frequency and acceleration for single-spring test cell. Lines show vibration conditions where piston transitions between up and down. Dashed lines are experimental data (O'Hern et al., 2016a), and solid lines are theoretical results (O'Hern et al., 2016a). Error bars indicate uncertainties of experimental data.

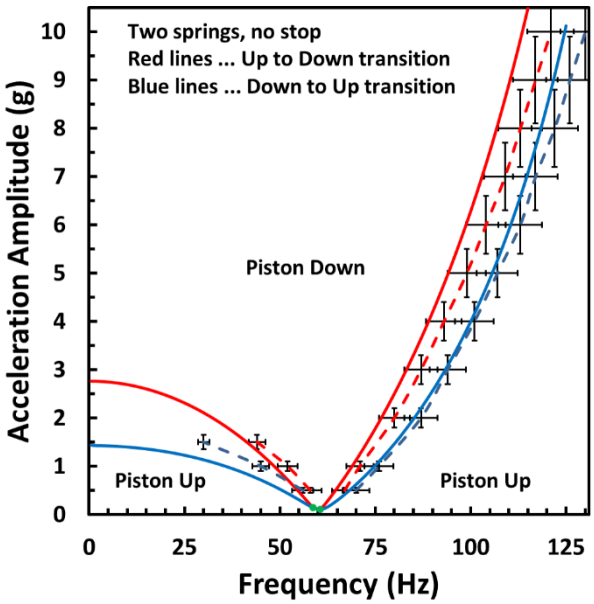

Figure 7. Regime map of piston equilibrium state (down or up) versus frequency and acceleration for two-spring test cell. Lines show vibration conditions where piston transitions from up to down (red) or down to up (blue). Dashed lines are experimental data, and solid lines are theoretical results (Torczynski et al., 2017). Error bars indicate uncertainties of experimental data.

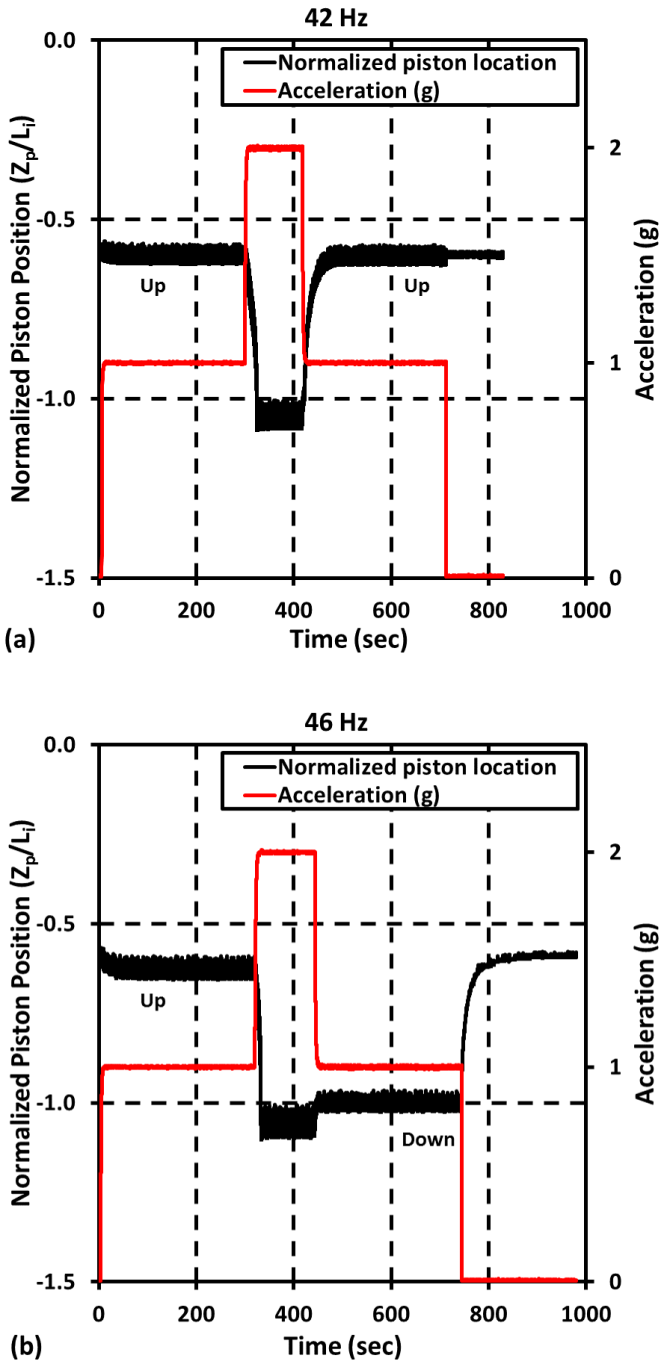

Figure 8. Normalized piston position vs. time at fixed frequency as acceleration is held fixed at 1g with a 120-s burst at 2g. Upper plot (a): at 42 Hz, after burst, piston returns to initial equilibrium position. Lower plot (b): at 46 Hz, after burst, piston finds new equilibrium position. Similar experiments are performed over ranges of acceleration and frequency to produce data in Fig. 9. (Piston position Z_P is normalized by maximum length of inner gap $L_I = 5.08$ mm .)

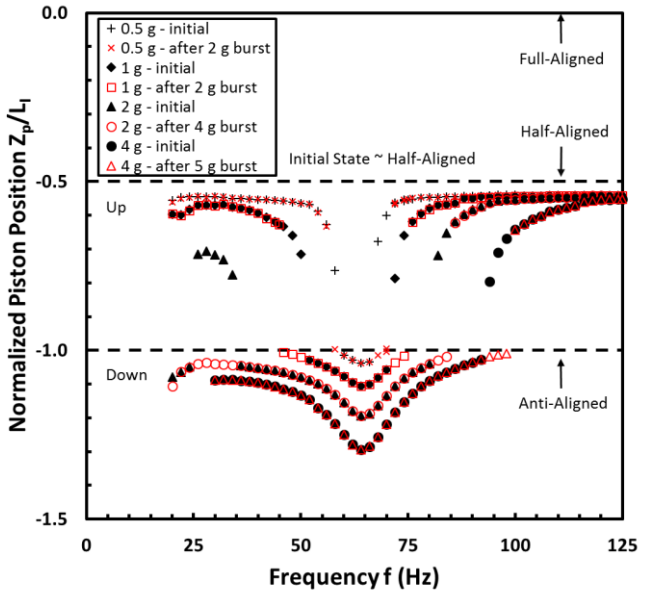

Figure 9. Equilibrium piston position versus frequency for fixed acceleration. Data are from experiments like those in Fig. 8. Black symbols are initial equilibrium positions, and red symbols are final equilibrium positions after brief burst of increased acceleration.

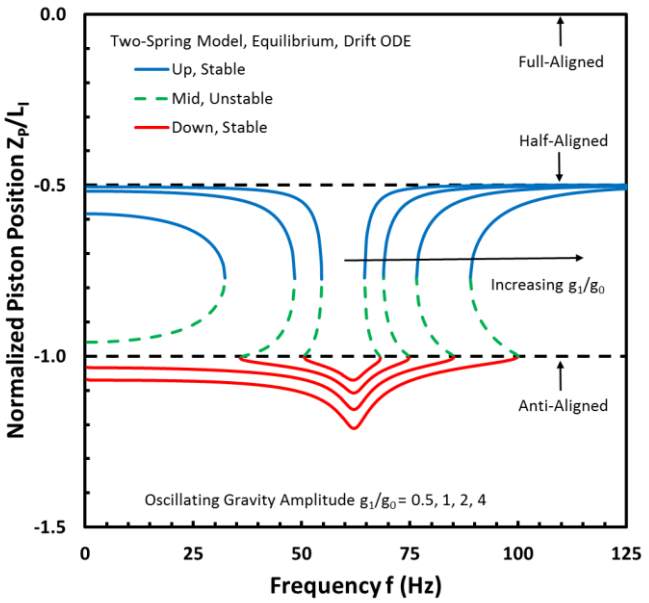

Figure 10. Theoretical equilibrium piston position vs. frequency from drift ODE model of Torczynski et al. (2017). Blue curves are stable up positions, red curves are stable down positions, and green curves are unstable middle positions. Accelerations are same as for experimental results in Fig. 9: 0.5g, 1g, 2g, and 4g.

Figure 7 shows similar data from the two-spring test cell indicating the measured vibration conditions at which the piston transitions from up to down or down to up. These experiments are run by holding the acceleration fixed, slowly changing the frequency in discrete steps (here, 1 Hz), allowing the piston to come to equilibrium, and measuring its position. Each discrete frequency is held for 5 minutes since piston motion from up (near half-aligned) to down (near anti-aligned) can be very slow (Torczynski et al., 2017). Upward and downward frequency sweeps are performed to determine the four critical frequencies that occur at a given acceleration. The blue dashed curves show the transition from an initial down state to a final up state, and the red dashed curves show the transition from an initial up state to a final down state. Figure 7 also shows corresponding theoretical results (Torczynski et al., 2017). Their analysis showed that, for a fixed acceleration, the piston remains in the up state at low and high frequencies, moves to the down state at intermediate frequencies, and can be in either the up state or the down state for narrow frequency bands separating these regions.

In Figs. 8-10, the piston position Z_P is normalized by the maximum length of the inner gap L_I (Torczynski et al., 2017). Thus, the normalized position is –0.5 for the initial half-aligned position and –1.0 for the anti-aligned position.

Figure 8 shows another type of experiment in the two-spring test cell to determine the equilibrium piston position as a function of the vibration conditions. In these experiments, the frequency is kept fixed, but the acceleration is fixed first at a lower value for 5 minutes, then increased to a higher value for 2 minutes (the "burst"), and then returned to its original lower value for the final 5 minutes. These experiments have two goals: to measure the equilibrium piston position for fixed vibration conditions, and to determine whether up and/or down states exist at each frequency. At some frequencies (e.g., 42 Hz in Fig. 8a), the piston returns to its initial up equilibrium position at 1g after the 2g burst. However, at other frequencies (e.g., 46 Hz in Fig. 8b), the piston transitions from its initial up equilibrium position at 1g to a final down equilibrium position at 1g after the 2g burst.

Figure 9 summarizes the results of many such experiments with the two-spring test cell at four different fixed accelerations (0.5g, 1g, 2g, and 4g) and frequencies of 20-125 Hz. Frequency ranges are observed within which the up state is the only stable equilibrium piston position, within which the down state is the only stable equilibrium position, and within which both positions are possible. In the latter situation, the equilibrium state achieved depends on how the given vibration conditions are approached. More specifically, if the piston position is above the up state, then the piston finds the up state, and if the piston is below the down state, then the piston finds the down state.

Figure 10 shows the corresponding theoretical results from Torczynski et al. (2017). The blue curves indicate the stable up states, the red curves indicate the stable down states, and the green curves indicate the unstable middle states. All three states exist in the middle-state frequency ranges. The experimental and theoretical results are seen to be in good agreement.

DISCUSSION

While overall trends are similar, the results in Fig. 6 and others like them show that a systematic difference exists between the single-spring experiments and the theory. In particular, the experimental data have a threshold for the acceleration, below which the piston does not move down. The single-spring test cell has a stop against which the piston is pushed by its spring, as in Fig. 1 and Fig. 2b. At this time, the theory and simulations do not consider this stop. Moreover, the single-spring experiments have poor repeatability. This may be due to interactions of the top of the piston with the stop when downward piston motion begins (e.g., asperity contact, squeeze-film damping, etc.).

To remove the effect of the stop, the two-spring test cell was built and employed to acquire the data sets shown in Figs. 7-10. Based on comparing Figs. 6-7, the single-spring and two-spring test cells have significantly different resonant frequencies: 107 Hz and 64 Hz, respectively. Different resonant frequencies are obtained for the two test cells because their spring constants and their total masses (piston plus liquid) differ appreciably.

All subsequent experiments used the two-spring test cell. Here, agreement with theory and repeatability of experimental results are both good. Figure 7 shows that the experimental and theoretical results for the down-to-up and up-to-down transitions are in essential agreement (the experiments could not be run at the lowest frequencies due to excessive vertical displacements). The experiments and theory show that, for a fixed acceleration, the piston moves to the up state (somewhat below half-aligned) at low and high frequencies, to the down state (somewhat below anti-aligned) at intermediate frequencies near resonance, and to either one state or the other in the frequency bands separating these regions.

Figure 9 shows the measured equilibrium piston positions for different vibration frequencies at fixed accelerations of 0.5g, 1g, 2g, and 4g. These data show the frequency ranges that have stable up and/or down equilibrium states and unstable middle equilibrium states. When two positions are possible, the state obtained depends on the initial condition. For example, at 1g acceleration, the up state is always achieved for frequencies of 36-44 Hz and 76-86 Hz, the down state is always achieved for frequencies of 54-70 Hz, and either the up state or the down state can be achieved for frequencies of 46-50 Hz and 72-74 Hz.

These frequency ranges are in good agreement with the theoretical results of Torczynski et al. (2017), shown in Fig. 10. The experimental data here are double-valued because the piston position under those vibration conditions depends on whether the piston is moving to its equilibrium position from a position near half-aligned or near anti-aligned. These double-valued regions correspond to the thin regions between the red and blue curves in Fig. 7. Similar results are seen for 0.5g acceleration, but the down state occurs over a smaller frequency range closer to resonance. For the 2g and 4g experiments, the range of down states extends further from resonance, and, for 4g, no up state exists for frequencies below resonance, in agreement with the theoretical results shown in Fig. 10.

CONCLUSIONS

We perform experiments to quantify how introducing a small amount of gas can cause large net (rectified) motion of a solid object in a vibrated liquid-filled housing when the drag on the object depends strongly on its position within the housing. Here, bellows are used as surrogate gas regions and form a well-characterized pneumatic spring against which the total mass (piston plus liquid) can oscillate. Adding this pneumatic spring to the original spring-mass-damper system allows the piston, the bellows, and the liquid to move together in a collective motion. This so-called Couette mode has low damping relative to the original Poiseuille mode and has a resonance near the frequency based on the pneumatic spring constant and the total mass.

Experiments are performed to investigate the dynamical behavior of this system. Two test cells are developed and used. The single-spring test cell has a lower spring that pushes the piston up against a stop. The two-spring test cell is basically the same as the single-spring test cell except that the upper stop is replaced by an upper spring.

Multiple experiments with both test cells are performed to measure the equilibrium piston position as a function of vibration conditions (frequency and acceleration). The experimental and theoretical results for the single-spring test cell show systematic differences apparently related to the interaction of the piston and the stop. This interaction is not considered in the theory and is not reproducible from day to day in the experiments. However, the two-spring experimental and theoretical results (Torczynski et al., 2017) agree quite well, indicating that the theory and the experiments include the dominant physics of vibration-induced piston motion in these systems. Future work will include a more detailed investigation of the effect of the stop on the initiation of piston motion and a more detailed study of bubble motion through narrow gaps under vibration.

ACKNOWLEDGMENTS

The authors gratefully acknowledge technical interactions with Gilbert L. Benavides and Louis A. Romero, now retired from Sandia National Laboratories. The authors also express their appreciation to Carlton F. Brooks and W. Marley Kunzler, of Sandia National Laboratories, for developing the LabVIEW data acquisition software used for these experiments.

Sandia National Laboratories is a multi-mission laboratory managed and operated by Sandia Corporation, a wholly owned subsidiary of Lockheed Martin Corporation, for the U.S. Department of Energy's National Nuclear Security Administration under contract DE-AC04-94AL85000.

This manuscript has been authored by Sandia Corporation under Contract No. DE-AC04-94AL85000 with the U.S. Department of Energy. The United States Government retains and the publisher, by accepting the article for publication, acknowledges that the United States Government retains a non-exclusive, paid-up, irrevocable, world-wide license to publish or reproduce the published form of this manuscript, or allow others to do so, for United States Government purposes.

REFERENCES

Asami, T., Honda, I., and Ueyama, A., 2014, "Numerical analysis of the internal flow in an annular flow channel type oil damper," *Journal of Fluids Engineering*, **136**(3), 031101, 1-8.

Bjerknes, V. F. K., 1906, *Fields of Force*, Columbia University Press, New York.

Clearco, 2017, Clearco Products, Willow Grove, PA, "Polydimethylsiloxane Properties," http://www.clearcoproducts.com/pdf/pure-silicone/polydimethylsiloxanes-properties.pdf.

O'Hern, T. J., Torczynski, J. R., and Clausen, J. R., 2016a, "Liquid-gas dynamic system under vibration," Proceedings of the 9th International Conference on Multiphase Flow.

O'Hern, T. J., Torczynski, J. R., and Clausen, J. R., 2016b, "Multiphase effects in dynamic systems under vibration," HTFEICNMM2016-1074, ASME, New York.

O'Hern, T. J., Torczynski, J. R., and Clausen, J. R., 2016c, "Nonlinear dynamics of a spring-supported piston in a vibrated liquid-filled housing: II. experiments," *Bulletin of the American Physical Society*, **61**(20), 175.

Romero, L. A., Torczynski, J. R., and von Winckel, G., 2014, "Terminal velocity of a bubble in a vertically vibrated liquid," *Physics of Fluids*, **26**(5), 053301, 1-32.

Romero, L. A., Torczynski, J. R., Clausen, J. R., O'Hern, T. J., and Benavides, G. L., 2016, "Gas-enabled resonance and rectified motion of a piston in a vibrated housing filled with a viscous liquid," *Journal of Fluids Engineering*, **138**(6), 061302, 1-19.

Servometer, 2015, Servometer Precision Manufacturing Group, LLC, Cedar Grove, NJ, http://www.servometer.com/wp-content/uploads/2015/03/Metal_bellows_brochure_16_page_Rev11.pdf.

Torczynski, J. R., Romero, L. A., Clausen, J. R., and O'Hern, T. J., 2014, "Vibration-induced rectified motion of a piston in a liquid-filled cylinder with bellows to mimic gas regions," *Bulletin of the American Physical Society*, **59**(20), 494.

Torczynski, J. R., O'Hern, T. J., and Clausen, J. R., 2015, "Adding some gas can completely change how an object in a liquid-filled housing responds to vibration," *Bulletin of the American Physical Society*, **60**(21), 554.

Torczynski, J. R., O'Hern, T. J., and Clausen, J. R., 2016, "Nonlinear dynamics of a spring-supported piston in a vibrated liquid-filled housing: I. analysis," *Bulletin of the American Physical Society*, **61**(20), 175.

Torczynski, J. R., O'Hern, T. J., Clausen, J. R., and Koehler, T. P., 2017, "Gas-induced motion of an object in a liquid-filled housing during vibration: I. analysis," FEDSM2017-69022, ASME, New York.